Investigation of hydrocarbon-plasma-generated carbon films by electron-energy-loss spectroscopy

J. Fink, Th. Müller-Heinzerling, J. Pflüger,* and B. Scheerer
Kernforschungszentrum Karlsruhe, Institut für Nukleare Festkörperphysik, Postfach 3640, D-7500 Karlsruhe, Federal Republic of Germany

B. Dischler, P. Koidl, A. Bubenzer, and R. E. Sah
Fraunhofer Institut für Angewandte Festkörperphysik, Eckerstrasse 4, D-7800 Freiburg, Federal Republic of Germany
(Received 30 April 1984)

The bonding in hard, hydrogenated, amorphous carbon films (*a*-C:H) prepared by plasma decomposition of benzene was investigated by high-resolution electron-energy-loss spectroscopy. In all as-grown films we find that one-third of the carbon atoms are trigonally bonded and two-thirds of the carbon atoms are tetrahedrally bonded. For the trigonally bonded part, the dielectric properties reveal a transformation from polymeric state for samples prepared with low ion energy to a more graphitic state for films prepared with higher ion energy. Upon annealing, the number of carbon atoms in sp^2 configuration increases. The graphitization of the films is observed in two steps at 200 °C and at 400 °C. A closing of the optical gap and a delocalization of the π electrons is observed between 400 °C and 600 °C.

I. INTRODUCTION

It has been known for about thirty years that "diamondlike" films based on carbon and hydrogen can be prepared via glow discharge decomposition of hydrocarbons.[1] Only recently these films have received considerable attention[2–8] due to their interesting properties like extreme hardness, high transparency in the infrared, good electrical insulation, and resistance to chemical attack. These properties of hydrogenated amorphous carbon, also called *a*-C:H in analogy to *a*-Si:H, are the result of the microstructure of these films, i.e., the type of bonding of the carbon atoms and the rôle of hydrogen incorporation. The microstructure of these *a*-C:H films is still a matter of continuing debate. The similarity of its properties to diamond suggests the possibility that all carbon atoms are tetrahedrally bonded and that the electrons of the carbon are therefore in an sp^3 configuration. In this model, we expect a random network structure similar to that of amorphous silicon. However, electron-energy-loss spectroscopy (EELS),[5] electron spin resonance (ESR) spectroscopy,[9] near edge absorption spectroscopy,[8,10] as well as electron diffraction[11] give clear evidence of the existence of trigonally bonded carbon with electrons in sp^2 configuration. Quite recently quantitative information on the ratio of sp^2 carbon to sp^3 carbon in *a*-C:H films has also been obtained by EELS,[10] by infrared spectroscopy,[12] and by optical spectroscopy.[13] An analysis, assuming *a*-C:H films to be composed of different components, was attempted by optical spectroscopy in the energy range 1.45–5 eV.[14] The aim of the present contribution is to give information on the microstructure of *a*-C:H films for various preparation conditions, as grown and annealed, by analyzing the dielectric properties of the films derived from electron-energy-loss spectra in a wide energy range (0.5–40 eV). Parts of this work together with extended x-ray absorption fine structure (EXAFS) spectra on *a*-C:H films have already been published in a short communication.[10]

II. EXPERIMENTAL

a-C:H films were deposited on NaCl substrates in a rf plasma sustained by benzene vapor.[3,15] The rf-powered substrate is subject to a negative dc self-bias V_B. In the discharge region the hydrocarbons are ionized and the positive particles are accelerated towards the substrate under the negative voltage V_B, thus forming *a*-C:H films. The kinetic energy of the ions is an important quantity as it determines many properties of the growing film. The mean kinetic energy has been shown[15] to be proportional to $V_B P^{-1/2}$, where P is the hydrocarbon pressure.

The deposition parameters of our samples for a given geometry of the preparation chamber are listed in Table I. All four samples had a thickness of about 1000 Å. Details of the sample preparation are described elsewhere.[15] The refractive index for $E=0.62$ eV was determined from thin-film-optical interferences observed in transmission and reflection on equivalent but thicker samples.[16] The densities of the *a*-C:H films were derived by weighing substrates before and after coating and dividing the difference by the known film volume. The relative concentration of bonded hydrogen has been determined from the integrated intensity of the CH stretch vibrational absorption band. An estimate of the total hydrogen content of one sample was made by an effusion technique. The hydrogen effusion rate as a function of temperature has been determined by sealing the *a*-C:H sample in a quartz ampoule and measuring the pressure increase.

For the EELS measurements, the films were floated off from the NaCl substrate in distilled water and were placed on standard electron microscope specimen grids. For comparison, an amorphous carbon sample was prepared

TABLE I. Parameters for the 4 *a*-C:H samples. V_B, negative self-bias; P, C_6H_6 pressure; ρ, density; C_H, hydrogen concentration; n, refractive index at 0.62 eV; E_g, optical gap; E_p, energy of $\sigma+\pi$ plasmon; d_1, d value corresponding to maximum in the diffraction pattern with lowest momentum transfer; C_{sp^2}, concentration of carbon atoms in sp^2 configuration.

Sample	V_B (V)	P (μbar)	$V_B P^{-1/2}$ (V μbar$^{-1/2}$)	ρ (g/cm^3)	C_H (at.%)	n	E_g (eV)	E_p (eV)	d_1 (Å)	C_{sp^2} (%)
1	200	32	35	1.49	60	1.78	2.05	22.8	5.1	39
2	400	50	57	1.50	50	1.82	1.60	22.9	6.0	39
3	800	36	133	1.59	40	1.93	1.20	23.4	5.1	34
4	1200	19	275	1.75	25	2.10	0.95	24.0	4.5	38

by evaporating carbon with an electron beam gun onto a Cu foil. The Cu foil was dissolved in a $FeCl_3$ solution and the sample was placed again on a standard electron microscope specimen grid. Heat treatments of the samples for temperatures up to 1000 °C were carried out at constant temperature for periods of 1—4 h in a vacuum of 10^{-9} Torr. The EELS spectra were measured at room temperature with a high-resolution 170-keV electron-energy-loss spectrometer, having variable energy and momentum resolution. The spectra shown here were measured with an energy resolution of 0.15 eV and a momentum resolution between 0.04 and 0.1 Å^{-1} with beam currents of about 10 nA.

III. RESULTS

Typical electron diffraction spectra with momentum transfer up to 6 Å^{-1} and energy loss equal zero taken with the electron-energy-loss spectrometer are shown in Fig. 1. For annealing temperatures below 800 °C broad maxima were observed in all cases. The positions of the maxima near 3 Å^{-1} and near 5.4 Å^{-1} are independent of the preparation conditions and annealing temperature. At higher temperatures these maxima get more and more pronounced and transform near 1000 °C into the (101) and the (112) reflections of graphite as shown in the upper part of Fig. 1. The low momentum transfer peak near 1.2 Å^{-1} is strongly dependent on preparation conditions and annealing temperature. In Table I the d_1 values corresponding to the momentum transfer of these maxima are listed for the samples. Except for sample 1, the d_1 values decrease with increasing density. For higher annealing temperatures the d_1 values strongly decrease and the maximum transforms near 1000 °C into the (002) reflex of graphite layers as shown in Fig. 1. This decrease of the d_1 value as a function of temperature is shown for sample 3 in more detail in Fig. 6. Two transition points near 220 and 400 °C are observed.

Electron-energy-loss spectra of sample 2 as prepared and for the two annealing temperatures $T=585$ and 1000 °C are shown in Fig. 2. In order to avoid contributions from surface losses and radiation losses, the spectra were taken at a momentum transfer of 0.1 Å^{-1}. The elastic line as well as the contributions from double scattering are subtracted. The most pronounced structure in these spectra is the $\sigma+\pi$ plasmon near 20 eV. With increasing annealing temperature, the $\sigma+\pi$ plasmon energy decreases as shown in Fig. 6 for sample 3. Sample 2 was in-

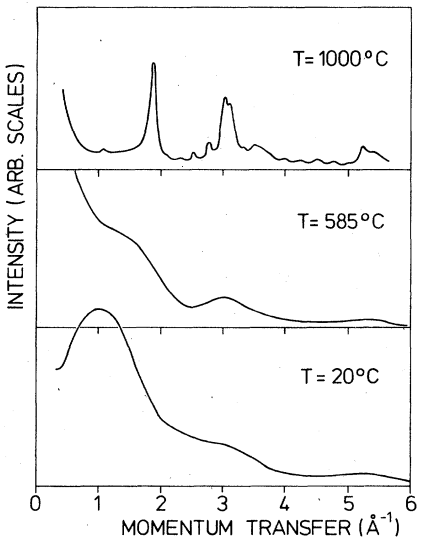

FIG. 1. Electron diffraction patterns of the *a*-C:H sample 2 as grown and for the annealing temperatures indicated, taken with the EELS spectrometer with energy loss equal to zero.

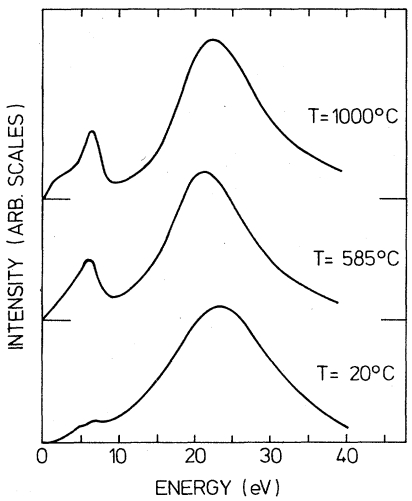

FIG. 2. Electron-energy-loss spectra taken with momentum transfer $q=0.1$ Å^{-1} on the *a*-C:H sample 2 as grown and for the annealing temperatures indicated.

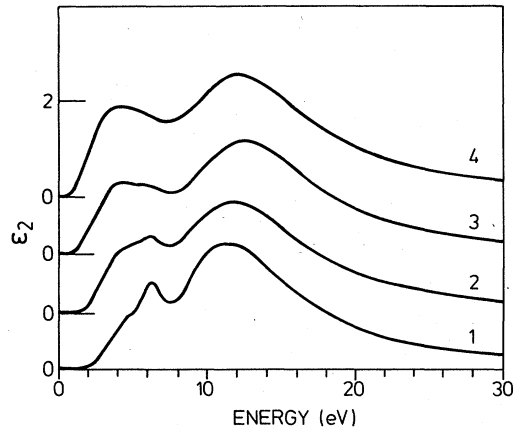

FIG. 3. Imaginary part of the dielectric function ϵ_2 for various a-C:H samples. The curves are labeled according to the sample number.

vestigated also at higher temperatures: above 700 °C the energy of the plasmon increases again. In the spectra shown in Fig. 2, a weaker second maximum near 6 eV is observed originating from excitations of π electrons. With increasing annealing temperature this maximum gets more and more pronounced. At $T=1000$ °C a strong π plasmon is observed as in graphite. For sample 2 we have measured the momentum dependence of the π excitations. Below about 500 °C no dispersion of the π excitations is observed. At 585 °C annealing temperature a dispersion coefficient $\alpha=0.25$ is obtained. α is defined by

$$E=E_0+\alpha(\hbar^2/2m)q^2 .$$

It is a measure of the delocalization of the π electrons. At $T=1000$ °C the dispersion coefficient reaches a value of 0.50.

In order to evaluate the dielectric functions from the measured loss spectra by a Kramers-Kronig analysis, we closely followed the procedure described by Daniels *et al.*[17] The absolute value of the loss function was deter-

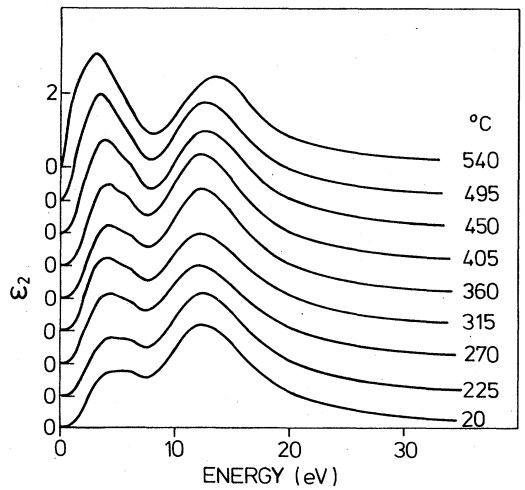

FIG. 4. Imaginary part of the dielectric function ϵ_2 for a-C:H sample 3 for annealing temperatures indicated.

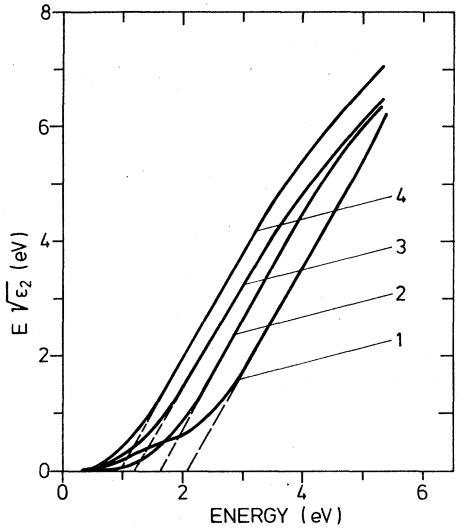

FIG. 5. Plot of $E\cdot(\epsilon_2)^{1/2}$ vs energy for various a-C:H samples. The curves are labeled according to the sample number.

mined using the refractive indices for $E=0.62$ eV as obtained by optical spectroscopy (see Table I). The dielectric functions are strongly dependent on preparation conditions. We only show the imaginary part ϵ_2 for the four samples in Fig. 3. As in graphite or in polymers with π electrons, there are two strong interband transitions contributing to ϵ_2, below 8 eV corresponding to π-π^* transi-

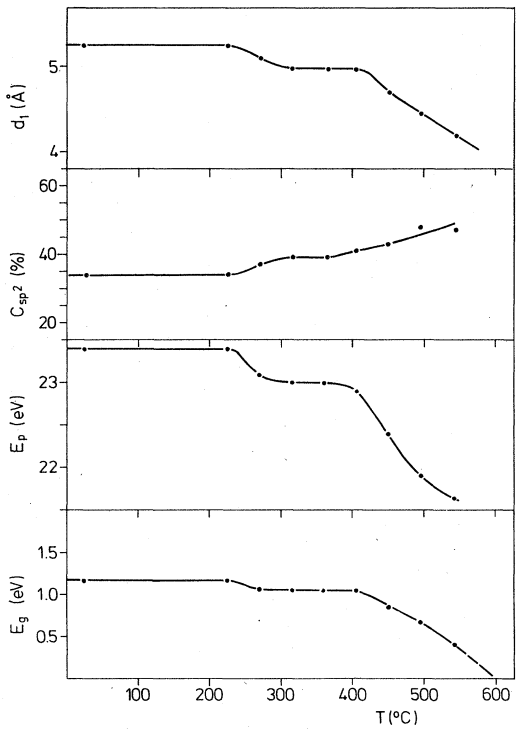

Fig. 6. Variation of parameters of a-C:H sample 3 as a function of the annealing temperature. d_1, d value corresponding to the diffraction peak with the lowest momentum transfer; C_{sp^2}, concentration of carbon atoms in sp^2 configuration; E_p, energy of the $\sigma+\pi$ plasmon; E_g, optical gap.

tions and above 8 eV corresponding to σ-σ^* transitions. With increasing kinetic energy of the ions in the preparation process, the oscillator strength of the π electron transitions increases. In Fig. 4 we show the imaginary part of the dielectric function for sample 3 at various annealing temperatures. The annealing time was 4 h for each temperature. With increasing temperature the oscillator strength of the π-electron transitions increases as well.

The optical gap E_g can be extracted from the energy dependence of ϵ_2 via the relation[18]

$$E\cdot[\epsilon_2(E)]^{1/2}=c\,(E-E_g)\,,$$

where c is a constant depending on the minimum metallic conductivity and the width of the tail-state region either at the top of the valence band or at the bottom of the conduction band. Although this relation is based on several approximations which might not be adequate for a-C:H films, it fits our data in a certain energy range as shown in Fig. 5. With increasing kinetic energy of the ions in the preparation process, the gap decreases. Values of the gap are listed in Table I. Similar curves were evaluated for annealed samples in order to get information as a function of annealing temperatures. The values extracted are shown in Fig. 6. Extrapolation of the data to higher temperatures yields a closing of the gap near 600 °C.

IV. DISCUSSION

We first discuss the influence of the preparation conditions on the properties of a-C:H films. There are two important parameters for the preparation, the negative self-bias voltage V_B and the benzene pressure P. The quantity $V_B P^{-1/2}$ is proportional to the mean kinetic energy of the ions impinging on the substrate.[15] It is this quantity which has proven to be the crucial parameter for many properties of the a-C:H films. For small $V_B P^{-1/2}$ (sample 1), one gets a polymerlike film having a small density, a low refractive index and a large gap of 2.05 eV as shown in Table I. We get more insight in the structure of this film by looking at ϵ_2 shown in Fig. 3(a). It is well known that for all pure hydrocarbons, interband transitions for energies less than about 8 eV correspond to transitions involving π electrons, whereas interband transitions with energies larger than 8 eV correspond to σ-σ^* transitions. For graphite, Taft and Philip[19] found π-π^* transitions at 4 eV and σ-σ^* transitions near 12 eV. The fact that strong interband transitions are found with energies less than 8 eV implies the presence of carbon atoms having π electrons, i,e., carbon atoms in sp^2 configuration. In order to obtain the effective number of π electrons and σ electrons per carbon atoms, the sum rule

$$N_{\text{eff}}=\frac{m}{2\pi^2 e^2 N}\int_0^{E_c} E\epsilon_2(E)dE$$

is evaluated, where N_{eff} is the effective number of electrons per atom contributing to interband transitions in the energy range 0 to E_c, N is the density of atoms and m is the electronic mass. Integrating up to 8 eV gives the number of carbon π electrons and integrating up to 40 eV gives the number of all electrons, the $\pi+\sigma$ electrons of carbon and the electrons of the hydrogen atoms forming a σ bond with the carbon atoms. For sample 2 the sum rule yields a ratio of π to $\sigma+\pi$ electrons of 0.08 which gives with a hydrogen concentration of 50 at. % a portion of 39% of the carbon atoms in the sp^2 configuration and the rest in sp^3 configuration having no π bonding. As an additional test we have also measured pure graphite films. Using the sum rule we obtain for the ratio $\pi/\sigma+\pi$ electrons the value $\frac{1}{4}$ in agreement with the results from optical spectroscopy.[19] For evaporated amorphous carbon films we get the same ratio indicating the nonexistence of carbon atoms in sp^3 configuration. Similar results have been obtained by neutron scattering by Mildner and Carpenter.[20] Looking in more detail on the structure of the π-π^* transitions in Fig. 3(1) the most pronounced maximum is near 6.5 eV which is close to the most prominent $^1A_{1g}$—$^1E_{1u}$ transition of benzene having an energy of 7 eV. A shoulder at lower energies is also observed in EELS spectra of oligomers of polyparaphenylen[21] which are chains of benzene rings. This low-energy transition is due to π electrons being delocalized over several benzene rings. Thus the low-energy part of ϵ_2 suggests that most of the carbon atoms in sp^2 configuration are bonded in benzene rings.

Increasing the energy of the ions in the preparation process reduces the intensity of the 6.5 eV maxima of ϵ_2 and increases the low-energy shoulder. For sample 4 having $V_B P^{-1/2}=275(V\,\mu\text{bar}^{-1/2})$ the π-π^* transitions show a peak near 4 eV as it is also observed in graphite. However, the width of the transition is strongly broadened in comparison with that of graphite. Going from sample 1 to sample 4, the portion of carbon atoms with sp^2 configuration does not change very much. However, other parameters show a considerable change. The density as well as the refractive index increases and the optical gap decreases as shown in Fig. 5 and in Table I. The values for the optical gap derived from EELS data are in excellent agreement with values derived from optical spectroscopy[15] on the equivalent samples. The content of bonded hydrogen is reduced by a factor of about 4. With increasing ion energy in the preparation process, the energy of the $\sigma+\pi$ plasmon increases. The energy of the plasmon should be[17]

$$E_P=\left[\frac{4\pi e^2\hbar^2}{m}n_{\text{eff}}\right]^{1/2},$$

with n_{eff} characterizing the density of electrons which participate in the plasmon resonance. Using the density and the hydrogen concentration given in Table I, good agreement of the calculated plasmon energy is obtained. Going to samples with higher refractive index, the density increases but the hydrogen content decreases and thus the calculated plasmon energy does not vary. For sample 4 we find a difference of 1.4 eV between the calculated and the experimental value of the plasmon energy. The origin of this discrepancy is not yet understood. The value for the first maximum in the diffraction patterns corresponding to the d_1 values shows a variation. These d_1 values

might be interpreted as distance between puckered carbon atom rings, as they approach at higher annealing temperatures the interplanar spacing of graphite planes. Going from sample 1 to sample 2 there is an increase in d_1 but then for higher ion energy d_1 decreases leading to a denser structure. All these variations of the measured parameters show a transition of the carbon atoms in sp^2 configuration from a polymerlike form with loosely bonded benzene rings with low density, high optical gap, and low refractive index to a more graphitic form with higher density, small optical gap, and higher refractive index. The complete transition to graphite was never observed in our samples prepared at room temperature. Also a plasmon near 34 eV corresponding to the diamond plasmon was never observed. This absence of diamondlike microstructure in our samples was also demonstrated recently by EXAFS measurements.[10] The ratio of carbon atoms in sp^2 configuration to those in sp^3 configuration in the room-temperature prepared samples was already published earlier.[10] Infrared spectroscopy measuring the stretch vibrations of H—C bonds and C—C bonds on equivalent samples[12] yields identical results, i.e., 68% sp^3 carbon for as grown samples. This indicates a homogeneous distribution of the hydrogen atoms on sp^3 carbon and sp^2 carbon. From optical spectroscopy McKenzie *et al.*[13] have deduced the presence of 0.47 π-bonded electrons per carbon atom in *a*-C:H films prepared from acetylene. This value is slightly higher than our value.

Annealing the films leads to a strong variation of most of the properties. The refractive index increases. Also all parameters derived from EELS measurements change for annealing temperatures higher than 220° as shown in Fig. 6. The d_1 value, interpreted as the mean distance of poorly ordered carbon planes decreases and merges into the d value corresponding to the interplanar spacing of graphite layers. The number of sp^2 carbon atoms increases and reaches about 50% near 500 °C. The optical gap decreases and closes near 600 °C. All these parameters show a variation corresponding to a transition into a more graphitic state. This view is also supported by looking at ϵ_2 plotted versus annealing temperature in Fig. 4. At low temperature, the 6.5 eV shoulder due to benzene rings is clearly detectable. At higher temperatures this shoulder disappears and the graphitic 4 eV π-π^* transition get more and more pronounced.

In graphite, the plasmon energy is observed at 27 eV. The variation of the plasmon energy upon annealing the samples is opposite to the expected direction. However, as the plasmon energy is proportional to the square root of the density of valence electrons, the decrease of the plasmon energy can be explained by a decrease of the density or by a release of hydrogen atoms. Assuming a release of all hydrogen without a change in density upon annealing up to 600 °C, an 11% and a 9% decrease of the plasmon energy is expected for sample 2 and sample 3, respectively. The experimental values for the two samples are 11% and 8%. This excellent agreement between calculated and experimental decrease of the plasmon energy upon annealing makes it highly probable that the variation of the plasmon energy is only caused by the hydrogen release at constant density. As we have not measured the density of our samples as a function of the annealing temperature we cannot exclude that the decrease of the plasmon energy is partially caused by a variation in density. In this context we mention that only minor changes of the density for annealing temperature less than 500 °C were observed by Smith.[14] At temperatures above 600 °C the plasmon energy increases again. For sample 2 a 1 eV increase was found between 600 and 1000 °C as can be seen in Fig. 2. This increase can be explained by an increasing density for higher annealing temperatures, also observed by Smith.[14]

The stepwise changes of all parameters at $T_a = 220$ °C and at $T_a = 400$ °C are not understood completely. Probably there exist two activation energies for the bonded hydrogen, leading to a step-wise release of hydrogen. In this interpretation a 20% hydrogen release has to be assumed near 220 °C, the rest is released between 400 and 600 °C. In fact a strong increase in the hydrogen effusion rate is observed at 500 °C with a maximum at 580 °C. The hydrogen release causes a transformation of H—C bonds into C=C double bonded carbon, increasing the number of sp^2 carbon atoms. This is observed in the C_{sp^2} values shown in Fig. 6.

At higher annealing temperature a pronounced π plasmon at 6 eV is found like in graphite. From the momentum dependence of the energy of the π plasmon, information on the delocalization of π electrons can be obtained. Excitations of localized electrons in narrow bands show no dispersion in momentum transfer whereas excitations of delocalized π electrons in wide bands show a large dispersion. For sample 2 and annealing temperatures less than 405 °C, the dispersion coefficient α is zero, indicating a complete localization of the π electrons. At $T_a = 585$ °C, $\alpha = 0.25$ is observed, i.e., between 400 and 585 °C a delocalization of π electrons occurs. This is consistent with the observation of the closing of the gap near 600 °C. Also, a strong increase in conductivity is found in this temperature region.[22] These results can be explained in terms of a simple percolation theory for π electrons already proposed by Gambino and Thomson.[9] The mean number of conductivity bonds per site must exceed a critical number for delocalization and thus conductivity to occur. A simple calculation gives that at least 50% of the carbon atoms must be sp^2 bonded to reach the critical concentration for delocalization of the π electrons. Our evaluation of the loss function yields a concentration of 50% sp^2 carbon near 500 °C as shown in Fig. 6 in excellent agreement with this model. Also infrared spectroscopy reveals a 50% concentration of sp^2 carbon in equally treated samples.[12] However, we do not want to conceal that a detailed comparison of the temperature dependence of the sp^2 carbon concentration shows differences between EELS data and infrared spectroscopy data for higher annealing temperatures.

At annealing temperature above 600 °C the dispersion coefficient increases indicating a broadening of the π band. For 1000 °C the dispersion coefficient α is found to be 0.5, which is very close to the value $\alpha = 0.55$ found for graphite. Thus for this annealing temperature, the band width of the π electrons is already very close to that of graphite.

V. CONCLUSIONS

The imaginary part of the dielectric function for *a*-C:H films as deduced from loss spectra gives information on the structure of the films. In all as-grown films, about one third of the carbon atoms is in the sp^2 configuration and two thirds is in sp^3 configuration. For small ion energies in the preparation process, most of the π electrons are localized in weakly bonded benzene rings, whereas for higher ion energies, π electrons are bonded in more graphitic rings. Upon annealing the films, a transformation to a graphitic state via two steps at 250 and 400 °C is found. The two steps are probably caused by two different activation energies for hydrogen release. As the number of carbon atoms in sp^2 configuration increases upon annealing, above 400 °C a percolation of π electrons with a delocalization of the π electrons is observed. The gap is closed near 600 °C. Above 600 °C, after hydrogen release, the transformation of the amorphous carbon to the graphitic structure is observed.

---

*Present address: Institute für Festkörperforschung, Kernforschungsanlage Jülich, Postfach 1913, D-5170 Jülich, Federal Republic of Germany.

[1]H. Schmellenmeier, Z. Phys. Chem. **205**, 349 (1955).
[2]D. A. Anderson, Philos. Mag. **35**, 17 (1977).
[3]L. Holland and S. M. Ojha, Thin Solid Films **38**, L17 (1976).
[4]H. Vora and T. J. Moravec, J. Appl. Phys. **52**, 6151 (1981).
[5]C. Weissmantel, K. Bewilogua, A. K. Breuer, D. Dietrich, U. Ebersbach, H.-J. Erler, B. Rau, and G. Reisse, Thin Solid Films **96**, 31 (1982).
[6]B. Dischler, A Bubenzer, and P. Koidl, Appl. Phys. Lett. **42**, 636 (1983).
[7]D. R. McKenzie, R. C. McPhedran, L. C. Botten, N. Sarvides, and R. P. Netterfield, Appl. Opt. **21**, 3615 (1982).
[8]D. Wesner, S. Krummacher, R. Carr, T. K. Sham, M. Strongin, W. Eberhardt, S. L. Weng, G. Williams, M. Howeks, F. Kampas, S. Hedd, and F. W. Smith, Phys. Rev. **28**, 2152 (1983).
[9]R. J. Gambino and J. A. Thomson, Solid State Commun. **34**, 15 (1980).
[10]J. Fink, Th. Müller-Heinzerling, J. Pflüger, A. Bubenzer, P. Koidl, and G. Crecelius, Solid State Commun. **47**, 687 (1983).
[11]D. R. McKenzie, L. C. Botten, and R. C. McPhedran, Phys. Rev. Lett. **51**, 280 (1983).
[12]B. Dischler, A. Bubenzer, and P. Koidl, Solid State Commun. **48**, 105 (1983).
[13]D. R. McKenzie, R. C. McPhedran, N. Savvides, and D. J. H. Cockayne, Thin Solid Films **108**, 247 (1983).
[14]F. W. Smith, J. Appl. Phys. **53**, 764 (1984).
[15]A. Bubenzer, B. Dischler, G. Brandt, and P. Koidl, J. Appl. Phys. **54**, 4590 (1983).
[16]O. S. Heavens, *Measurements of Optical Constants of Thin Films,* edited by G. Hass and R. E. Thun (Academic, New York, 1964), Vol. 2, p. 193.
[17]J. Daniels, C. V. Festenberg, H. Raether, and K. Zeppenfeld in Springer Tracts in Mod. Phys. **54**, 77 (1970).
[18]J. Tauc, R. Grigorovic, and A. Vancu, Phys. Status Solidi **15**, 627 (1966).
[19]E. A. Taft and H. R. Phillipp, Phys. Rev. **138**, A197 (1965).
[20]D. F. R. Mildner and J. M. Carpenter, J. Non-Cryst. Solids **47**, 391 (1982).
[21]J. Fink, G. Crecelius, J. J. Ritsko, M. Stamm, H. J. Freund, and H. Gonska, J. Phys. (Paris) Colloq. **44**, C3-741 (1983).
[22]B. Meyerson and F. W. Smith, J. Non-Cryst. Solids **35&36**, 435 (1980).